

# Process, microstructure and properties of squeeze-cast short-carbon-fibre-reinforced aluminium-matrix composites

C. P. JU, K. I. CHEN, J. H. CHERN LIN

*Department of Materials Engineering, National Cheng-Kung University, Tainan 70101, Taiwan*

Two types of high-modulus short-carbon-fibre-reinforced commercially pure aluminium-matrix composites were fabricated in-house using a home-made squeeze caster. The type-I composites were fabricated from short-fibre preforms in which fibres exist as dispersed bundles. The type-II composites were fabricated from preforms in which individual fibres were uniformly dispersed. The detailed processes are described in the text. A three-point-bending strength of higher than 200 MPa was obtained for the type-I composite with 17 vol% of fibre. When more fibre was incorporated, both the strength and the ductility decreased due to inadequate infiltration. However, a bending strength of greater than 240 MPa was recorded on a hot-rolled type-I composite with a fibre content as high as 28 vol%. This significant improvement in the mechanical properties is explained by a hot-rolling-induced *void-healing* effect. The type-II composites, with lower fibre volume fractions than those of the type-I due to their different preforms, exhibited bending strengths up to 166 MPa. Scanning electron microscopy fractography shows that the two types of composites fracture in distinctive manners. Transmission electron microscopy results featured thermal-stress-induced dislocations at carbon–aluminium interfaces as well as submicrometre-sized aluminium carbide, the reaction product, which nucleated from the interface and grew into the matrix interior.

## 1. Introduction

It is known that many properties of metal-matrix composites (MMCs) (such as high- and low-temperature specific strengths and moduli, wear resistance, toughness, thermal and mechanical fatigue resistance and creep resistance), are superior to monolithic metals and alloys [1]. In other properties (including high-temperature and transverse mechanical properties; thermal and electrical conductivity; and resistance to moisture, flames and radiation) MMCs are better choices than polymer-matrix composites [2]. MMCs have now been applied in the aerospace, satellite and automotive industries [3].

Among the many possible reinforcing materials, carbon fibres (note that the term *carbon fibre* is used throughout this paper to include both high-temperature-processed containing more graphitic fibres and lower-temperature processed containing less graphitic fibres) have advantages due to their light weight, high specific modulus and strength (depending on the type of fibre), high thermal and electrical conductivities and low coefficient of thermal expansion (CTE) in the fibre direction [4]. As a matrix material in MMCs, aluminium and its alloys are just as useful as in their monolithic forms. Carbon-fibre-reinforced aluminium and aluminium alloys have been fabricated in different ways [5–10] and they have been proved to be one of the most promising MMC systems.

In the present work two types of high-modulus short-carbon fibre-reinforced aluminium–matrix composites were fabricated in-house using a home-made squeeze caster. The microstructure, the properties and the process details of these composites are discussed.

## 2. Raw materials

A commercial aluminium with a purity higher than 99.5% and a high-modulus Courtaulds Grafil (Courtaulds Advanced Materials, UK) HM-370 PAN (polyacrylonitrile)-based carbon fibre were used as the major raw materials for fabrication of the present C/Al composite. Some properties of the fibre are listed in Table I. The surface is microscopically quite rough, as shown in Fig. 1, and this is considered beneficial to the bonding between carbon fibre and the aluminium matrix which usually do not bond as well as in other

TABLE I Properties of Courtaulds Grafil HM-370 fibre

Tensile strength	3.2 GPa
Tensile modulus	390 GPa
Elongation	0.8%
Density	1870 kg m <sup>-3</sup>
Filament diameter	6.5 µm
Number of filaments in a single yarn	12 000

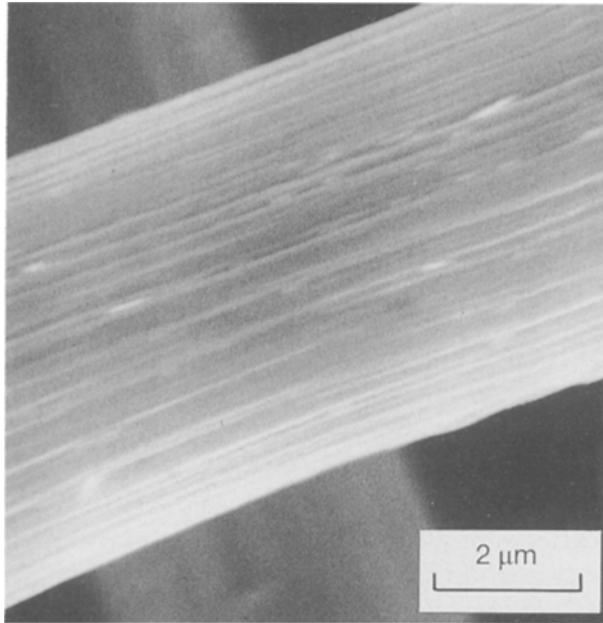


Figure 1 The SEM surface topography of the Grafil HM-370 fibres.

aluminium–matrix composites such as  $\text{Al}_2\text{O}_3/\text{Al}$  and  $\text{SiC}/\text{Al}$ . Since this study was focused only on the interaction between aluminium and carbon, a pure aluminium, rather than an aluminium alloy, was used as the matrix material. The only element intentionally added to the matrix to enhance wetting was Pb, as will be discussed later.

### 3. Short-fibre preforms

The as-received fibre yarns were cut into 3–5 mm short fibres, which were then ultrasonically dispersed in water containing 10 vol% of sodium silicate. In order to compare the composites with two remarkably

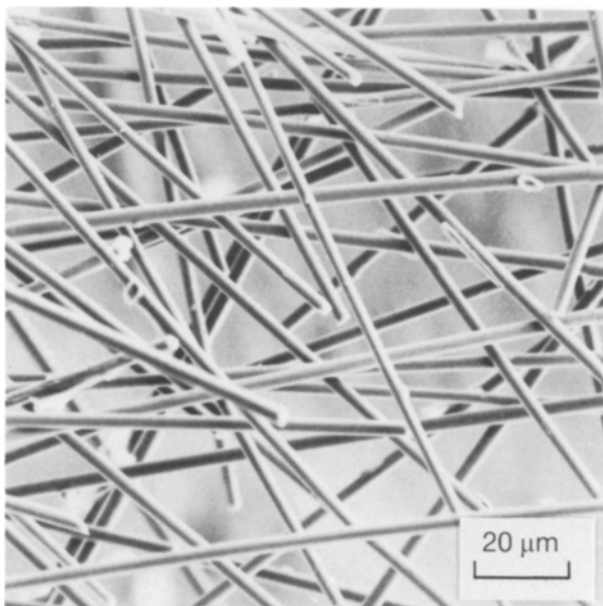


Figure 2 A SEM micrograph of well-dispersed short fibres.

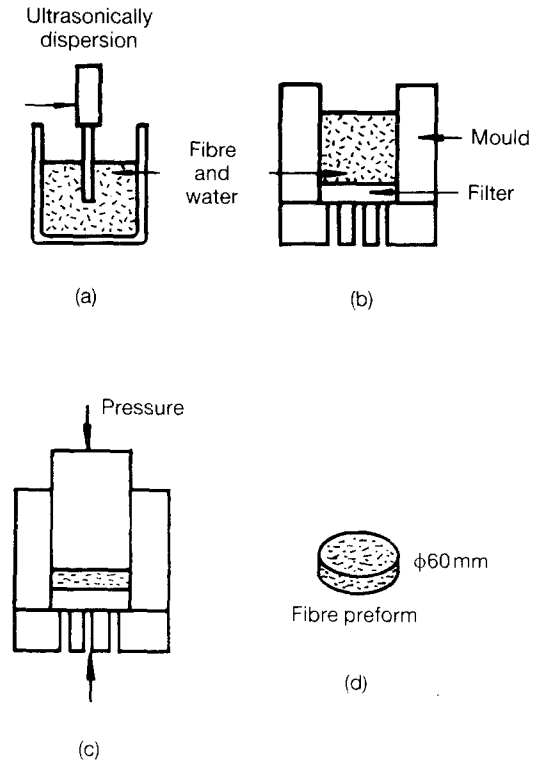


Figure 3 The process of manufacturing the fibre preforms.

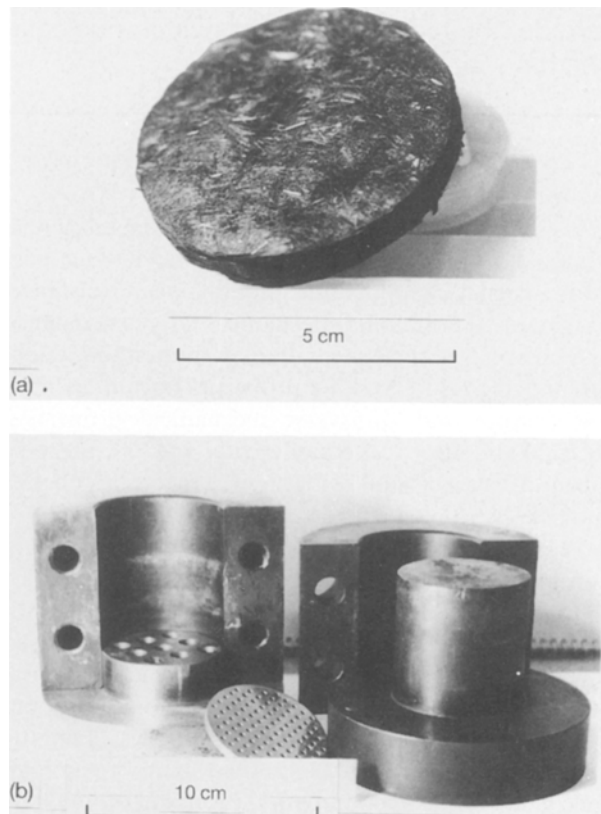


Figure 4 (a) A press-formed fibre preform, and (b) the mould used.

different types of fibre distribution, two dispersion times, 10 s and 2 min, were selected. With a 10 s dispersion the fibre bundles were dispersed, but fibres within each bundle still stuck together. The composite

fabricated from this type of fibre was designated the *type-I composite*. In contrast, with a 2 min dispersion, the fibre bundles were readily disassembled and the individual fibres were uniformly distributed, as shown in Fig. 2. The composite fabricated out of this type of fibre was designated the *type-II composite*. The ultrasonically dispersed short fibres were press-formed into 60 mm diameter preforms according to the process depicted in Fig. 3. A fibre preform prepared by this process and the mould used for the press-forming are shown, respectively, in Fig. 4a and b.

#### 4. Squeeze casting

The squeeze-casting process used for fabrication of the present C/Al composites is illustrated in Fig. 5. The mould for the casting was made of SKD61 tool steel and it had the same dimensions as the mould used in the preparation of the preforms. To facilitate the removal of castings from the mould, a thin layer of graphite powder was sprayed, prior to casting, onto the inner wall of the mould.

The casting temperatures were selected by considering the fact that too high a casting temperature causes a severe reaction between carbon fibres and molten aluminium, whereas too low a temperature would result in insufficient bonding. To assist the infiltration of the molten aluminium among individual fibres, the preforms needed to be preheated. In the present study the preheating temperatures were selected by considering the fact that too low a preheating temperature could not effectively help infiltration because of fast cooling of the melt, whereas too high a temperature (higher than about 600 °C) would cause noticeable oxidation of the carbon fibres.

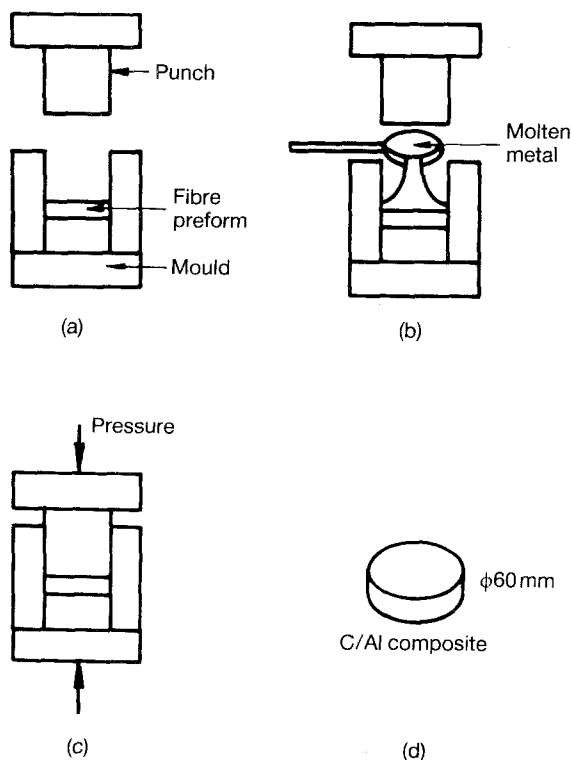


Figure 5 The process of squeeze casting.

The casting and preform preheating temperatures for the present type-I composite were in the ranges 770–810 °C and 500–520 °C, respectively, whereas for the type-II composite the respective temperatures were 820 °C and 550 °C. In squeeze casting of all composites, a pressure of 100 MPa was exerted and maintained until the molten aluminium was completely solidified. According to Zhu [11], a pressure of 100 MPa raises the melting temperature of aluminium by 10–25 °C. The reason that higher casting and preheating temperatures were used for the type-II composite was that the infiltration of molten aluminium among the well-dispersed fibres in this type of composite was more difficult. This phenomenon has been discussed by Li *et al.* [12]. Since it has been suggested that the addition of such alloying elements as Bi, Pb and Tl is capable of lowering the surface tension of molten aluminium [13], one per cent (in weight) of lead was added to the melt in this study. This addition of lead proved to be effective in improving the carbon–aluminium bonding and the composite strength.

Three type-I composites with different fibre contents (that is, 17, 21 and 27 vol %) as well as one type-II composite (with 11 vol % of fibre) were fabricated. While the pressure was kept the same in the preparation of fibre preforms, the density of the type-II preform was always much lower than that of the type-I preform due to the higher degree of fibre dispersion in the type-I preform. Consequently, a lower fibre content was obtained in the type-II composite when the pressures were fixed in the preparation of the preforms and in the squeeze casting. For comparison, pure aluminium was also squeeze-cast using similar process parameters.

#### 5. Mechanical properties

The mechanical properties of the squeeze-cast C/Al composites were evaluated by three-point-bending tests which were performed on an Instron 8500 IX system following the method described in JIS R1601.

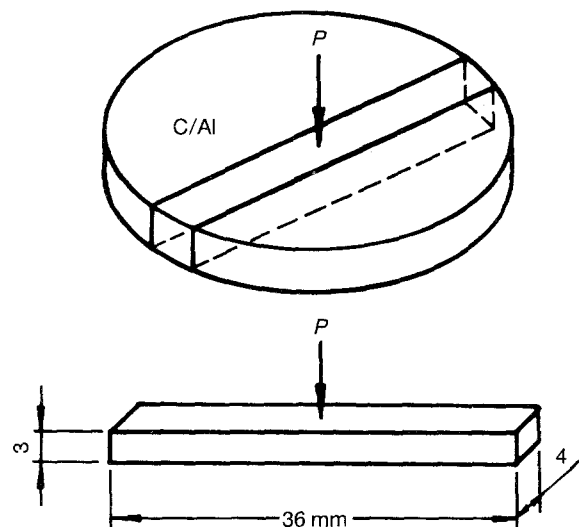


Figure 6 The composite specimen used for the bending test.

A ramp speed of  $0.5 \text{ mm min}^{-1}$  was used for all the tests. The composite coupons for the testing were machined from the squeeze-cast discs shown in Fig. 6. The bending strength was obtained from the equation  $S = 3PL/2WT^2$  ( $S$  in MPa) where  $P$  is the maximum load exerted,  $L$  is distance between the two supporting points,  $W$  is the specimen width (4 mm) and  $T$  is the specimen thickness (3 mm).

Table II lists bending properties of the typical-condition composites as well as of pure aluminium for comparison. These *typical* process conditions were different for the different types of composites, as described in Section 4. For the type-I composites, the bending strength and strain (at maximum load) were both found to decrease with the fibre content from, respectively, 209 MPa and 1.67% for 17 vol % of fibre to 164 MPa and 0.77% for 21 vol % of fibre, and down to 149 MPa and 0.56% for 27 vol % of fibre. This decrease in both the strength and strain with the fibre content is explained by the deterioration in infiltration and fibre–matrix bonding which occurred in the composites containing more fibres, as will be shown in Section 6.

As mentioned earlier, the infiltration of molten aluminium was less effective in the type-II composites than in type I. This was because, for the type-I composites, the molten aluminium could more easily penetrate into the preform interior through inter-bundle channels. For the type-II composites, on the other hand, the fibres were so uniformly dispersed that fairly open interbundle channels did not exist and, consequently, preforms (and also composites) with lower volume fractions of fibre were produced using the same process parameters. As shown in Table II the type-II composite with 11 vol % of fibre had a bending strength comparable to that of the type-I composite with 21 vol % of fibre. This is because worse bonding between aluminium and individual fibres (due to a less thorough infiltration within the fibre bundles) occurred in the type-I composite with 21 vol % of fibre. As discussed earlier, the casting and preform preheating temperatures could not be raised (to enhance infiltration) without taking into account the oxidation of molten aluminium and/or carbon fibre. In this study, compromises had to be made in the selection of these temperatures.

One of the type-I composites was further hot rolled at  $500^\circ\text{C}$  by a gross reduction of 33% in thickness.

TABLE II Three-point-bending properties

Material	$V_f$ (vol %)	Strength (MPa)	Strain at maximum load (%)
Type I	17	209	1.67
Type I	21	164	0.77
Type I	27	149	0.56
Type I <sup>a</sup>	28	242	0.91
Type II	11	166	1.83
Aluminium	0	~ 53	> 2.0
Aluminium <sup>b</sup>	0	~ 87	> 2.0

<sup>a</sup>Hot-rolled.

<sup>b</sup>Mould preheated at a lower temperature.

This composite with 28 vol % fibre had a bending strength of 242 MPa and strain at maximum load of 0.91% after rolling. This significant improvement in mechanical properties, compared to those of as-cast samples with comparable fibre volume fractions, can be primarily attributed to a hot-rolling-induced “healing” effect. During this healing (hot rolling) process, many pre-existing voids/pores were ironed out by the high-temperature plastic deformation. The microstructure of such hot-rolled composites will be shown later. Although a thorough study in this area was not attempted, the potential to improve the properties of squeeze-cast C/Al composites by a thermo-mechanical approach is obvious.

As a reference, pure aluminium was squeeze cast into moulds preheated at two different temperatures. The aluminium cast into the mould preheated at  $520^\circ\text{C}$  (similar to that for the type-I composite) had a bending strength of only 53 MPa. The aluminium cast into the lower temperature ( $440^\circ\text{C}$ ) mould had a strength of about 87 MPa due to its finer grain structure.

## 6. Microstructure

The overall distribution of fibres and the extent of the infiltration of aluminium, particularly among individual fibres, was evaluated by optical microscopy (OM). Specimens for OM were prepared following the usual metallographic procedure through a final level of  $0.3 \mu\text{m}$  alumina powder. The fracture surfaces of the composites were examined using a JEOL JSM-35 scanning electron microscope. More detailed microstructural information, particularly in the fibre–matrix reaction zone, was obtained from a Hitachi-H700 transmission electron microscope operated at 200 kV. Thin foils for TEM were prepared by mechanical dimpling of the press-drilled 3 mm diameter discs to a central thickness of less than  $50 \mu\text{m}$ , followed by argon-ion milling until perforation.

Optical micrographs of type-I composites containing 17, 21 and 27 vol % of fibre are given in Fig 7. It can be clearly seen that in type-I composites carbon fibres are embedded in the aluminium matrix in the form of flattened bundles as a result of the squeeze-casting process. In the composite with 17 vol % fibre (Fig. 7a) the aluminium thoroughly penetrated into each bundle and it was well-bonded to every single fibre. In the composite with 21 vol % of fibre (Fig. 7b), however, many microvoids were observed under the optical microscope. These microvoids existed at the fibre–matrix interface, particularly between two fibres which closely neighboured each other. In the composite with 27 vol % of fibre (Fig. 7c) the infiltration was even worse. This is why in this fibre-volume-fraction range the bending strength of the type-I composites decreased when more fibres were introduced.

The microstructure of the hot-rolled type-I composite with 28 vol % fibre is shown in Fig. 8. The absence of the voids observed in the as-cast type-I composites with high volume fractions of fibre indicated that the aluminium-depleted spots had been “healed”

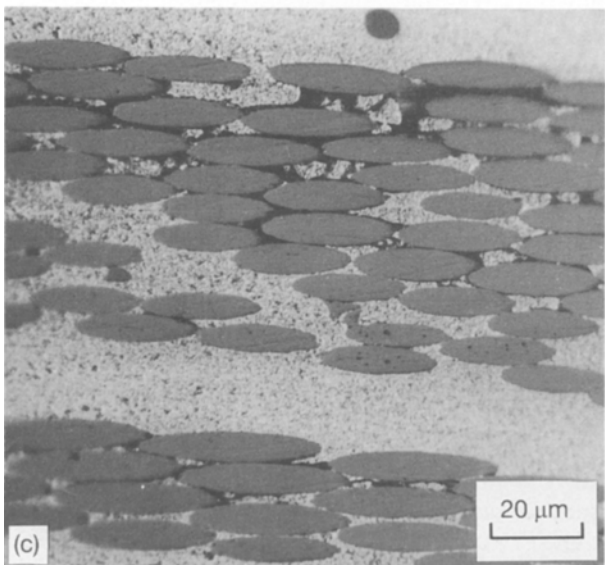
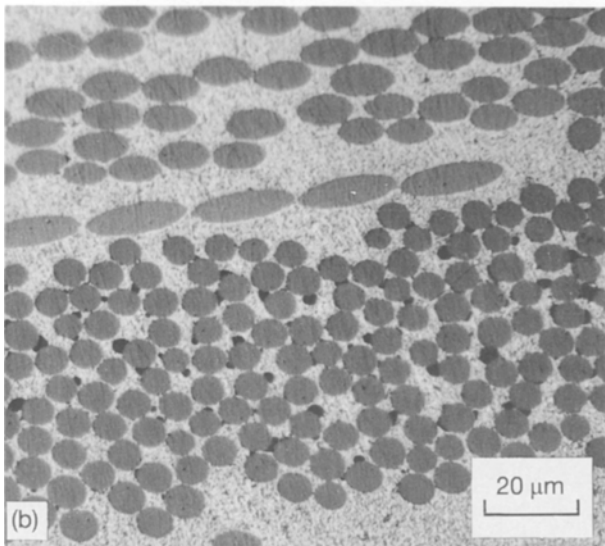
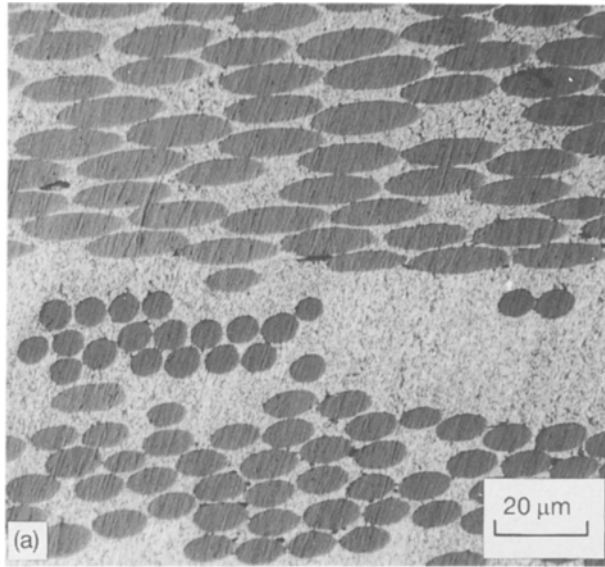


Figure 7 Optical micrographs of type-I composites with: (a) 17 vol %, (b) 21 vol %, and (c) 27 vol % of fibre.

by the high-temperature plastic deformation process, as discussed earlier. This is believed to be the major reason for the large improvement of the mechanical properties of this composite after hot rolling. Work

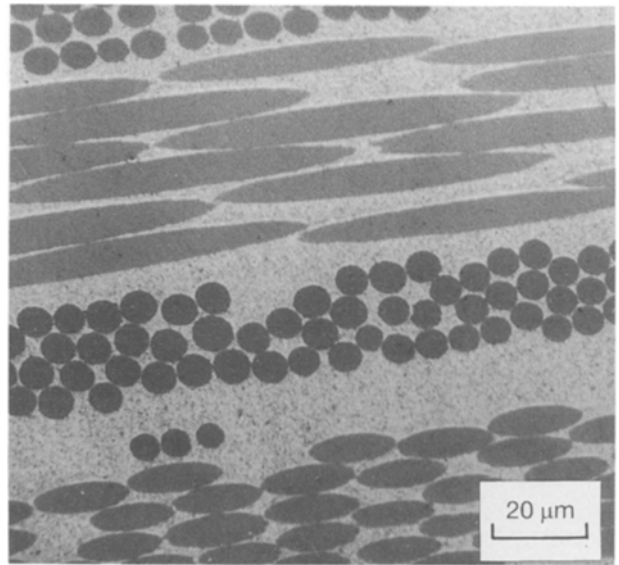


Figure 8 An optical micrograph of a hot-rolled type-I composite with 28 vol % fibre.

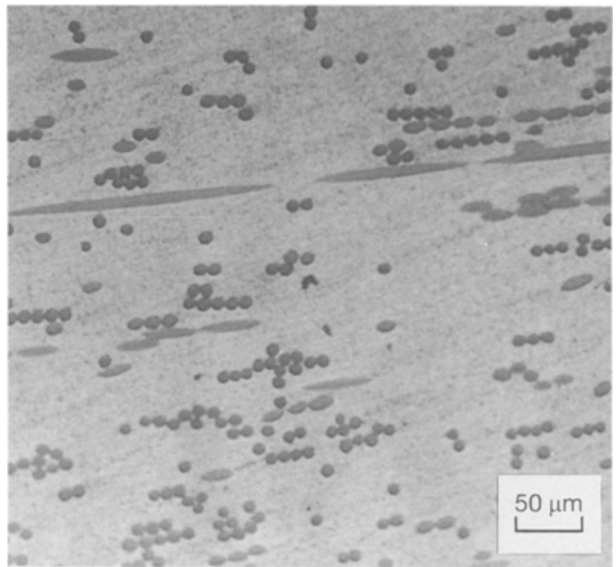


Figure 9 An optical micrograph of a type-II composite with 11 vol % of fibre.

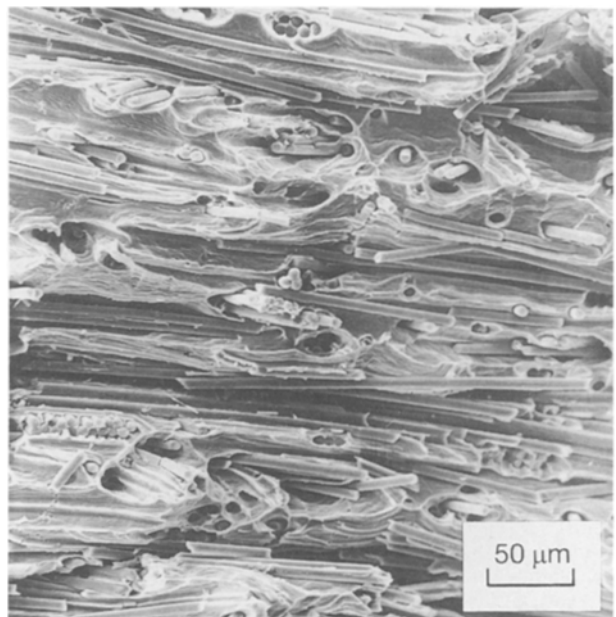


Figure 10 A SEM fractograph of a type-II composite with 11 vol % of fibre.

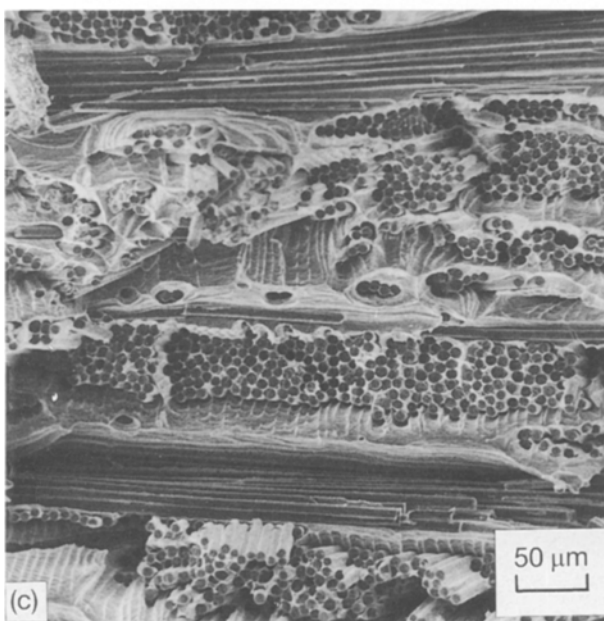
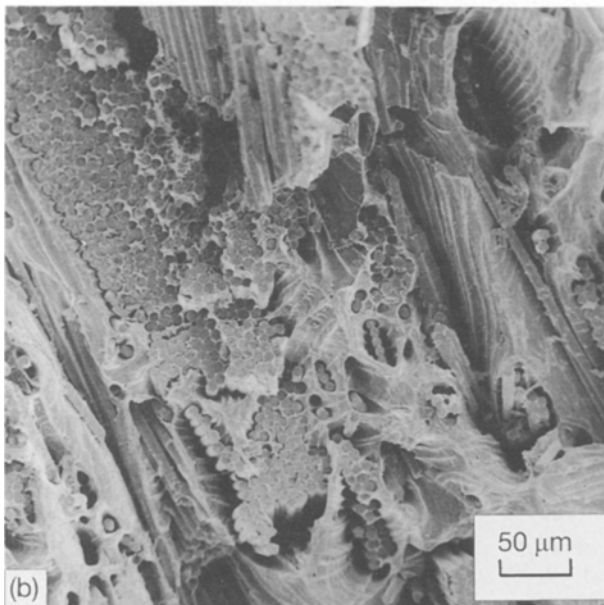
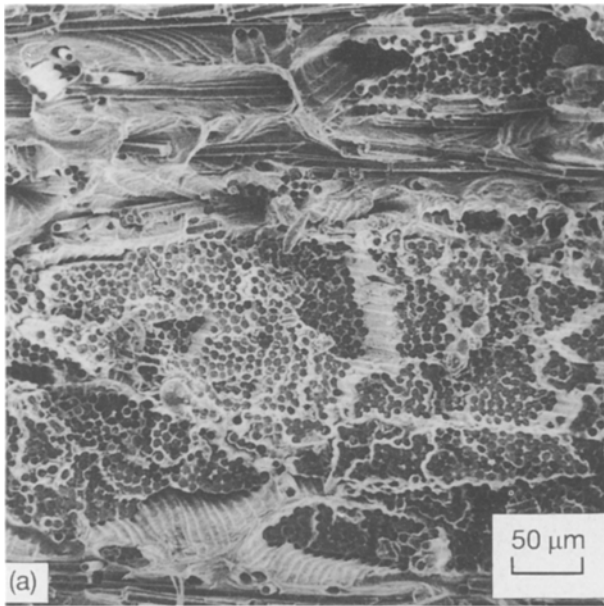


Figure 11 SEM fractographs of type-I composites with (a) 17 vol %, (b) 21 vol %, and (c) 27 vol % of fibre.

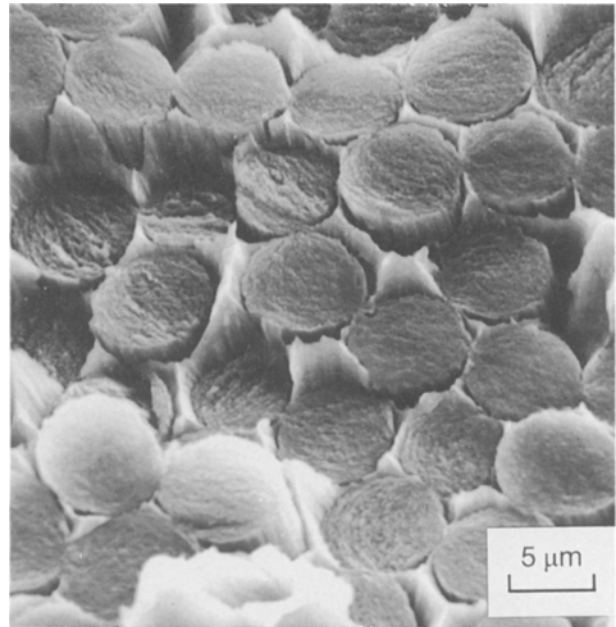


Figure 12 A SEM fractograph of a hot-rolled type-I composite with 28 vol % of fibre.

hardening of the aluminium matrix, another possible contributing factor, is not considered as critical in this case due to the high-temperature at which the rolling was carried out.

In the type-II composite with 11 vol % of fibre, fibre bundles were disassembled and individual fibres were dispersed, although small-sized clusters comprising up to tens of fibres still existed, as shown in Fig. 9. Microvoids were observed inside some of these clusters. The scanning electron micrograph taken from the fracture surface of this composite (shown in Fig. 10) showed that the aluminium matrix experienced heavy plastic deformation, whereas the quite uniformly distributed carbon fibres had been broken, partially debonded or completely pulled out. Compared to this, the fracture surface of type-I composites looked much different. As shown in the examples in Figs 11 and 12, the overall fracture surface of the type-I composites was rough as a result of uneven fracture of fibre bundles. Within each bundle the brittle fractured fibres were still bonded by the matrix. Gaps were often observed between the matrix and the fibre bundles. The matrix aluminium appeared to have experienced less plastic deformation than in the more ductile type-II composite. The higher magnification fractograph of a single bundle shown in Fig. 12 clearly shows that molten aluminium had filled each open space among the individual fibres. In the course of fracture, most fibres became separated from their surrounding matrix aluminium, leaving between them a submicrometre-wide interfacial gap. The fracture surface of each fibre featured a typical brittle-failure pattern of high-modulus carbon fibres.

To obtain microstructural information in more detail, the type-I composite with 17 vol % fibre was examined by TEM. A typical morphology of the fibre-matrix interfacial region in this composite is shown in the bright field (BF) micrograph in Fig. 13a.

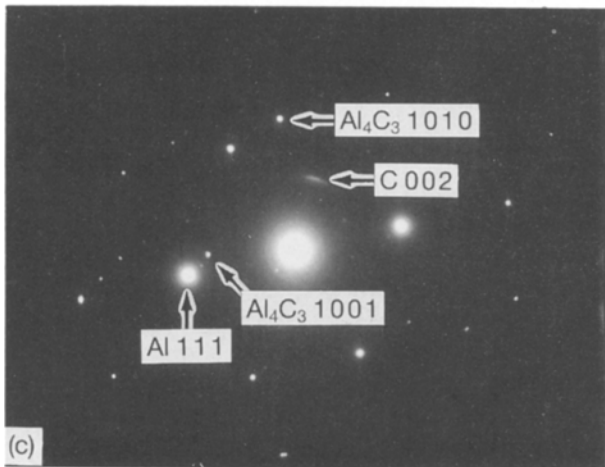
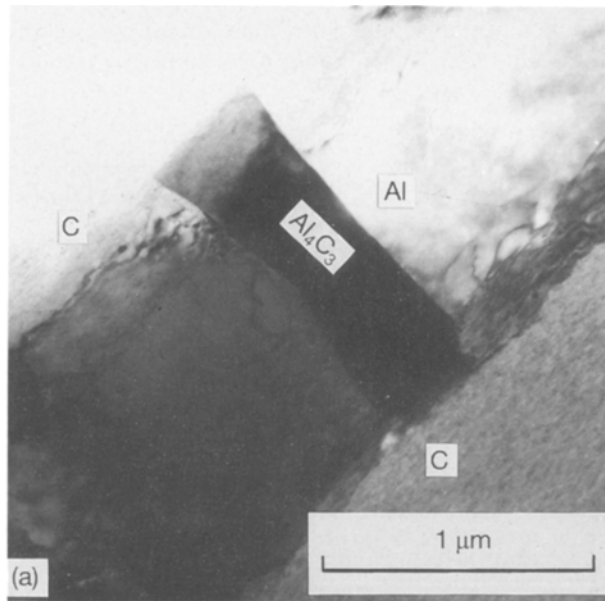


Figure 13 (a) A TEM bright-field micrograph, (b) a selected-area diffraction pattern and (c) its index of a type-I composite with 17 vol % of fibre.

Due to the large difference in the CTE between carbon fibres and aluminium, thermal stresses were induced during cooling of the composite. Such stresses could easily initiate dislocations at the fibre–matrix interface, as shown in Fig. 13a. These thermal-stress-induced dislocations are frequently observed in as-cast as well as in thermally cycled carbon- or ceramic-fibre-

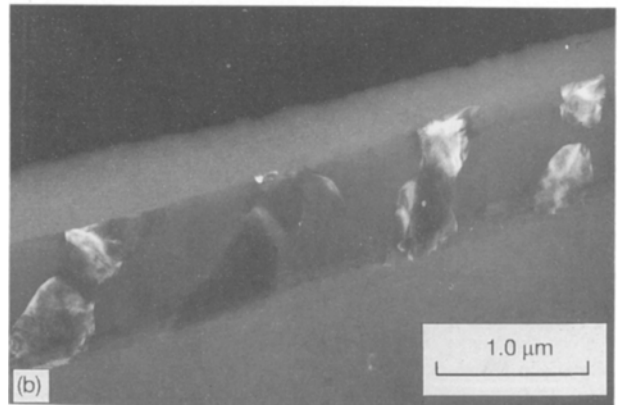
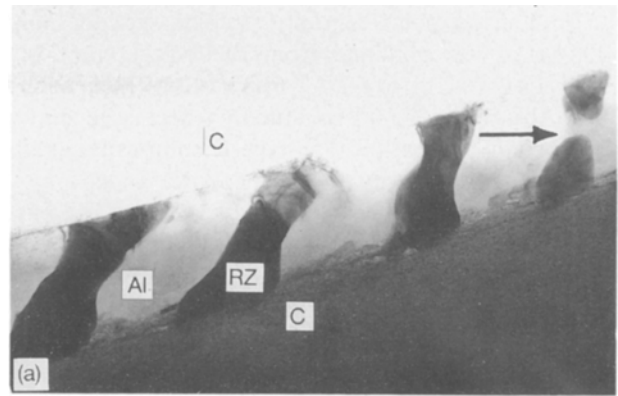


Figure 14 (a) A TEM bright-field and (b) a dark-field micrograph of a type-I composite with 17 vol % of fibre.

reinforced light-metal composites such as alumina-fibre-reinforced aluminium and magnesium alloys [14]. The submicrometre-sized reaction product,  $\text{Al}_4\text{C}_3$ , obviously nucleated from the carbon–aluminium interface (note the arrowed region in Fig. 14) and grew into the matrix interior. The dark-field (DF) micrograph imaged out of an aluminium-carbide diffraction spot, Fig. 14b, indicates that those dark carbide particles observed in the BF image were by no means single crystals. Instead, they were composed of many smaller grains within each particle.

An interesting observation, shown in Fig. 14, was that carbide particles, which had nucleated on opposite sides of two neighbouring fibres and which had grown mutually into the matrix between them, tended to merge in to each other and they eventually turned into single particles. This argument is supported by the fact that each carbide particle has a neck somewhere in the middle of its length. The reasons why the two sets of particles had to merge into each other one-on-one and why these particles have similar spacings are not certain at this time.

## 7. Conclusions

1. Two types of short-carbon-fibre-reinforced aluminium composites were fabricated in-house using a squeeze-casting technique. In the type-I composites, fibres existed as bundles, whereas in the type-II composites the fibres were fully and individually dispersed. The type-I composites had higher fibre volume fractions than those of the type-II in the present processes.

2. A three-point-bending strength greater than 200 MPa was obtained from the type-I composite with 17 vol % of fibre. As more fibres were added, both the strength and the ductility decreased due to inadequate infiltration. The type-II composites exhibited bending strengths up to 166 MPa.

3. A strength of greater than 240 MPa was obtained from a hot-rolled type-I composite with a fibre content as high as 28 vol %; this can be explained by a hot-rolling-induced "void-healing" effect.

4. SEM fractography showed that in the type-I composites whole fibre bundles fracture in an uneven manner, whereas in the type-II composites individual fibres were broken, debonded or pulled out. The matrix aluminium in type-I composites experienced less plastic deformation than that in the more ductile type-II composites.

5. TEM revealed that thermal-stress-induced dislocations were generated at the fibre-matrix interface as a result of the large difference in the CTE between carbon fibres and aluminium. The submicrometre-sized reaction product,  $Al_4C_3$ , nucleated from the carbon-aluminium interface and grew into the matrix interior. Each aluminium-carbide particle contained many smaller grains.

### Acknowledgements

The authors are grateful to the National Science

Council of the Republic of China for support for this research under contract No. NSC 80-0405-E006-39.

### References

1. J. E. SCHOUTENS, in "Reference book for composites technology", Vol. 1, edited by S. M. Lee (Technomic, Lancaster, PA, 1989) p. 175.
2. K. K. CHAWLA, in "Composite materials science and engineering" (Springer-Verlag, New York, 1987) p. 89.
3. R. B. ARONSON, *Machine Design* **8** (1985) 68.
4. J.-B. DONNET and R. C. BANSAL, in "Carbon fibres" (Marcel Dekker, New York, 1990) p. 267.
5. E. G. KENDALL, in "Composite materials", Vol. 4. Metallic matrix composites, edited by K. G. Kreider (Academic Press, New York and London, 1974) p. 319.
6. I. H. KHAN, *Met. Trans. A* **7** (1976) 1281.
7. A. K. JHA, S. V. PRASED and G. S. UPADHYAYA, *Tribology Int.* **22** (1989) 321.
8. P. R. GIBSON, A. J. CLEGG and A. A. DAS, *Mater. Sci. Technol.* **1** (1985) 559.
9. R. J. SAMPLE, R. B. BHAGAT and M. F. AMATEAU, in "Cast reinforced metal composites", edited by S. G. Fishman and A. K. Dhingra (American Society for Metals, Metals Park, Ohio, 1988) p. 93.
10. A. P. DIWANJI and I. W. HALL, in *ibid.* p. 225.
11. Z. ZHU, in *ibid.* p. 93.
12. H. LI, Z. MAO, B. SHANG and Y. ZHOU, *Acta Materialia Composita Sinica* **8** (1991) 21.
13. G. L. RANSHOFEN, *Aluminium* **49** (1973) 231.
14. C. P. JU, unpublished research.

Received 13 May 1993

and accepted 6 January 1994